

# The complement: a solution to liquid drop finite size effects in phase transitions

L. G. Moretto<sup>1</sup>, K. A. Bugaev<sup>1</sup>, J. B. Elliott<sup>1</sup>, R. Ghetti<sup>2</sup>, J. Helgesson<sup>3</sup> and L. Phair<sup>1</sup>

<sup>1</sup>*Nuclear Science Division, Lawrence Berkeley National Laboratory, Berkeley, CA 94720*

<sup>2</sup>*Department of Physics, Lund University, Sweden*

<sup>3</sup>*School of Technology and Society, Malmö University, Sweden*

(Dated: November 1, 2019)

The effects of the finite size of a liquid drop undergoing a phase transition are described in terms of the complement, the largest (but still mesoscopic) drop representing the liquid in equilibrium with the vapor. Vapor cluster concentrations, pressure and density from fixed mean density lattice gas (Ising) model calculations are explained in terms of the complement. Accounting for this finite size effect is key to determining the infinite nuclear matter phase diagram from experimental data.

PACS numbers:

Finite size effects are essential in the study of nuclei and other mesoscopic systems for opposite, but complementary reasons. In modern cluster physics, the problem of finite size arises when attempts are made to relate well known properties of the infinite system to the cluster properties brought to light by experiments [1]. For nuclear physics, the problem is the opposite: finite size effects dominate both the macroscopic and spectroscopic physics at all excitation energies and the challenge is to reduce the vast amount of specific knowledge of each “drop” (nucleus) to a general characterization of uncharged, symmetric infinite nuclear matter. This reduction has been achieved thus far, only for cold nuclei by determining the saturation binding energy and density in terms of the liquid drop model. Finite size effects are also encountered in nuclear physics in efforts to generate a liquid-vapor phase diagram from heat capacity measurements [2] and fragment distributions [3].

We present here a general approach to deal with finite size effects in phase transitions and illustrate it for liquid-vapor phase coexistence. A dilute, nearly ideal vapor phase is in equilibrium with a dense liquid-like phase; finiteness is realized when the liquid phase is a finite drop. The vapor pressure of a finite drop, different than that of the infinite liquid, was calculated by correcting the molar vaporization enthalpy to include the surface energy of the drop [4, 5]. We introduce the concept of the complement (the residual drop remaining after a cluster has been emitted) to extend and quantify finite size effects down to drops as small as atomic nuclei. We generalize Fisher’s model [6], deriving an expression for individual cluster concentrations of a vapor in equilibrium with a finite drop and then recover the Gibbs-Thomson formulae [8] as a limiting case. We demonstrate our approach with the lattice gas (Ising) model.

The complement method consists of evaluating the change in free energy occurring when a cluster is moved from one phase to another. In the case of a finite liquid drop in equilibrium with its vapor, this is done by transferring a cluster of any given size from the liquid drop to its vapor and by evaluating the energy and entropy

changes associated with *both* the vapor cluster *and* the residual liquid drop (complement). This accounting can be generalized to incorporate other energy terms common in the nuclear case, e.g. symmetry energy, Coulomb energy (with caution [7]) and even angular momentum.

We examine the vapor within the framework of physical cluster theories for non-ideal vapors, which assume that the monomer-monomer interaction is exhausted by the formation of physical clusters. The concentrations of clusters of  $A$  constituents  $n_A(T)$  depend on the free energy of cluster formation  $\Delta G_A(T) = \Delta E_A(T) - T\Delta S_A(T)$ . The epigon of these theories is Fisher’s model [6] which writes, at coexistence,  $\Delta E = c_0 A^\sigma$  and  $\Delta S_A(T) = \frac{c_0}{T_c} A^\sigma - \tau \ln A$ . The cluster concentration is

$$n_A(T) = \exp \left[ -\frac{\Delta G_A(T)}{T} \right] = q_0 A^{-\tau} \exp \left( -\frac{c_0 A^\sigma \varepsilon}{T} \right) \quad (1)$$

where  $q_0$  is a normalization,  $\tau$  is Fisher’s topological exponent,  $c_0$  is the surface energy coefficient,  $\sigma$  is the surface to volume exponent, and  $\varepsilon = (T_c - T)/T_c$ . The leading term in  $\Delta S_A(T)$ , proportional to  $A^\sigma$ , permits the vanishing of the cluster free energy at a  $T = T_c$  independent of size. Equation (1) (and the extension below) is valid only at phase coexistence for  $T \leq T_c$ . The direct physical interpretation of the parameters in  $\Delta G_A(T)$  and their application to the nuclear case is the reason for this choice here, despite its limitations [9].

We now generalize Eq. (1), valid for a vapor in equilibrium with the infinite liquid, to the case of a vapor in equilibrium with a finite liquid drop. Consider a vapor in equilibrium with a drop of its liquid. For each cluster of the vapor we can perform the gedanken experiment of extracting it from the liquid, determining the change in entropy and energy of the drop and the cluster, and then putting it back into the liquid (the equilibrium condition), as if, according to physical cluster theories, all other clusters of the vapor did not exist. Fisher’s expressions for  $\Delta E_A(T)$  and  $\Delta S_A(T)$  can now be written for a drop of size  $A_d$  in equilibrium with its vapor as  $\Delta E_A(T) = c_0 [A^\sigma + (A_d - A)^\sigma - A_d^\sigma]$  and  $\Delta S_A(T) = \frac{c_0}{T_c} [A^\sigma + (A_d - A)^\sigma - A_d^\sigma] - \tau \ln [A(A_d - A)/A_d]$ . The

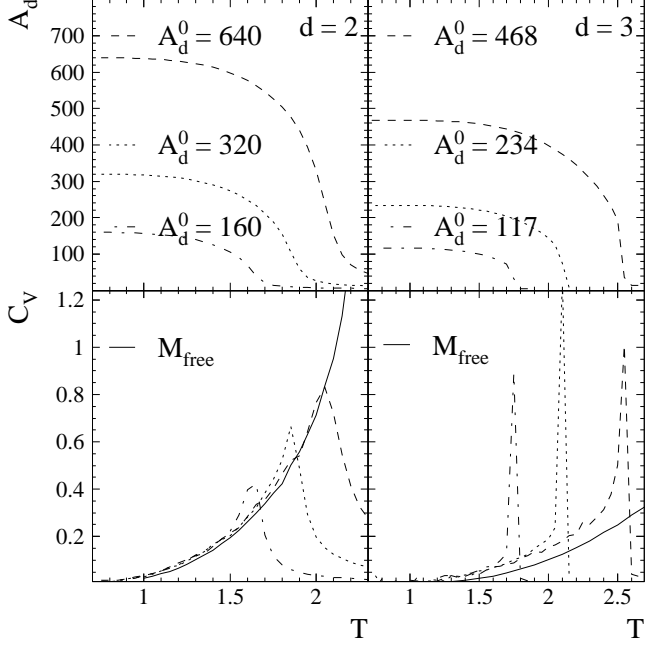


FIG. 1: On the left (right), top to bottom: the  $d = 2$  ( $3$ ) liquid drop size  $A_d$ , specific heat  $C_V$ . See text for details.

cluster concentration is then

$$n_A(T) = q_0 \left[ \frac{A(A_d - A)}{A_d} \right]^{-\tau} \exp \left\{ -\frac{c_0 \varepsilon}{T} [A^\sigma + (A_d - A)^\sigma - A_d^\sigma] \right\}. \quad (2)$$

We treat the free energy cost of forming the complement ( $A_d - A$ ) in a similar fashion as the free energy cost of forming a cluster. The resulting expression reduces to Eq. (1) when  $A_d$  tends to infinity. While different than the standard Fisher expression, Eq. (2) still contains exactly the same parameters as that of the infinite system. We can rewrite Eq. (2) in the following form

$$n_A(T) = n_A^\infty(T) \exp \left( \frac{A \Delta \mu_{fs}}{T} \right) \quad (3)$$

with  $n_A^\infty(T)$  given by Eq. (1). The finite size of the drop acts as an *effective* chemical potential,  $\Delta \mu_{fs} = -\{c_0 \varepsilon [(A_d - A)^\sigma - A_d^\sigma] - T \tau \ln [(A_d - A)/A_d]\}/A$ , increasing the vapor pressure [8].

In order to quantitatively demonstrate this method, we apply it to the canonical lattice gas (Ising) model [14, 15] with a fixed number of up spins, i.e. the fixed mean occupation density  $\rho_{\text{fixed}}$  lattice gas (equivalently, the fixed magnetization  $M_{\text{fixed}}$  Ising model) [18]. Up spins represent lattice sites occupied by particles of the fluid forming monomers, dimers, large drops etc. Down spins are empty space; the lattice is the container enclosing the fluid. We choose lattices large enough that, when coupled with periodic boundary conditions, minimize finite

lattice effects, irrelevant to our study. For  $d = 2$  ( $3$ ) we use a square (simple cubic) lattice of side  $L = 80$  ( $25$ ) which, with periodic boundary conditions, leads to a shift in  $T_c$  of  $\lesssim 0.5\%$  [11, 12] ( $\lesssim 0.5\%$  [13]). The  $M_{\text{fixed}}$  calculations were performed via the geometric cluster method [17]. For every temperature  $T$  and  $\rho_{\text{fixed}}$ , over  $10^5$  thermalized realizations were generated to produce the cluster concentrations. We performed  $M_{\text{free}}$  calculations for the same lattices as a benchmark in order to differentiate between the effects of a finite lattice and of a finite drop.

For the  $M_{\text{fixed}}$  calculations at  $T = 0$ , the up spins congregate into a single liquid drop in a vacuum: the ground state. At higher temperatures, the vacuum is filled with a vapor made up of up spin clusters. Clusters in the vapor were identified via the Coniglio-Klein algorithm [19] to insure that their behavior is physical (i.e., cluster concentrations return Ising critical exponents and not percolation exponents). The largest cluster represents the liquid drop and is identified geometrically (all like spin nearest neighbors bonded) in order to capture the skin thickness associated with liquid drops [18]. Our choices of ground state liquid drops  $A_d^0$  (shown in Fig. 1) are similar in size to large atomic nuclei and insure that, for the lattices enclosing them, the ground state is approximately circular (spherical) for the  $d = 2$  ( $3$ ) lattices used. Due to periodic boundary conditions the drop's ground state shape can change with  $M_{\text{fixed}}$  [16].

Figure 1 shows that as  $T$  increases, the drop's size  $A_d$  decreases from  $A_d^0$ : an evaporating drop fills the container with vapor. At temperature  $T_X$ , corresponding to the end of two phase coexistence,  $A_d$  falls quickly. The value of  $T_X$  varies with  $A_d^0$ . For  $T \lesssim T_X$  the specific heat  $C_V$  (measuring spin-spin interaction energy fluctuations only) agrees approximately with the  $M_{\text{free}}$  results (solid lines in Fig. 1) for all  $A_d^0$  until fluctuations in  $A_d$  at  $\sim T_X$  produces a  $C_V$  greater than that of the  $M_{\text{free}}$  results. As  $T$  increases further,  $C_V$  decreases.

To evaluate the efficacy of the complement, we examine the scaled cluster concentrations for our calculations:  $n_A(T)/q_0 A^{-\tau}$  vs.  $c_0 A^\sigma \varepsilon / T$ . For  $M_{\text{free}}$  calculations it has been shown that this scaling collapses concentrations of clusters over a wide range in  $A$  and  $T$  [9]. Finite size liquid drop effects will be manifested in the cluster concentrations of the  $M_{\text{fixed}}$  calculations which should scale better according to Eq. (2) rather than to Eq. (1).

Only clusters of  $A \geq 9$  are used in the  $M_{\text{free}}$  fits for the  $d = 2$  calculations. This is because only large clusters obey Fisher's ansatz for the cluster surface energy:  $E_A = c_0 A^\sigma$ . Small clusters are dominated by geometrical shell effects [21]. For the  $d = 3$   $M_{\text{fixed}}$  calculations, large clusters are very rare, so clusters of  $A \geq 2$  are used in our analysis. Thus, the magnitude of the resulting  $\chi^2$  values from the  $d = 3$  calculations are due to the clusters analyzed not closely following Fisher's ansatz.

In the thermodynamic limit, the highest temperature admitted by Eq. (1) or (2) is the temperature at which

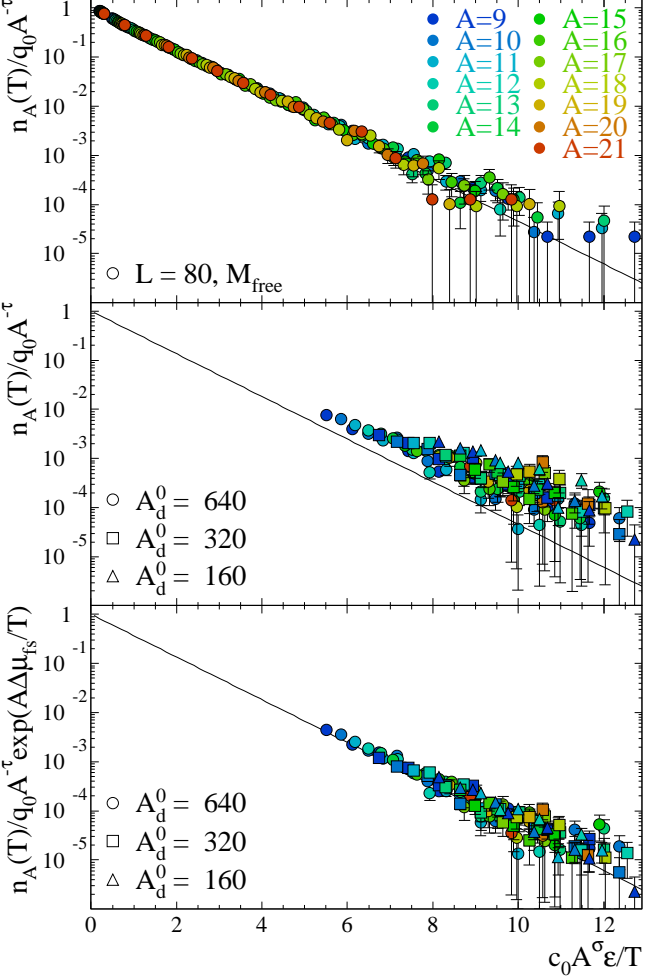


FIG. 2: [Color online] The cluster concentrations of the  $d = 2$ ,  $L = 80$  periodic boundary condition square lattice for:  $M_{\text{free}}$  calculations (top);  $M_{\text{fixed}}$  calculations with no complement (middle);  $M_{\text{fixed}}$  calculations with the complement (bottom).

TABLE I: Fit results for  $M_{\text{free}}$  calculations

-	Onsager	this work	theoretical values	this work
-	$d = 2$	$d = 2$	$d = 3$	$d = 3$
-	$L \rightarrow \infty$	$L = 80$	$L \rightarrow \infty$	$L = 25$
$\chi^2_\nu$	-	4.7	-	1972.2
$T_c$	2.26915	$2.283 \pm 0.004$	$4.51152 \pm 0.00004$	$4.533 \pm 0.002$
$c_0$	$\geq 8$	$8.6 \pm 0.2$	$\geq 12$	$12.63 \pm 0.04$
$\sigma$	$8/15$	$0.56 \pm 0.01$	$0.63946 \pm 0.00008$	$0.725 \pm 0.003$
$\tau$	$31/15$	$2.071 \pm 0.002$	$2.209 \pm 0.006$	$2.255 \pm 0.001$

the system leaves coexistence. For the  $M_{\text{free}}$  calculations this occurs at  $T = T_c$ , while for the  $M_{\text{fixed}}$  calculations this occurs at  $T \approx T_X$ . However, due to the small size of our drops, fluctuations grow large before  $T_X$ . Thus we limit our fit up to a temperature  $T_{\text{fit}} < T_X$ : for  $d = 2$   $T_{\text{fit}} = 1.6$ , 1.5 and 1.4 for  $A_d^0 = 640$ , 320 and 160, respectively; for  $d = 3$   $T_{\text{fit}} = 1.7$ , 1.5 and 1.3 for  $A_d^0 =$

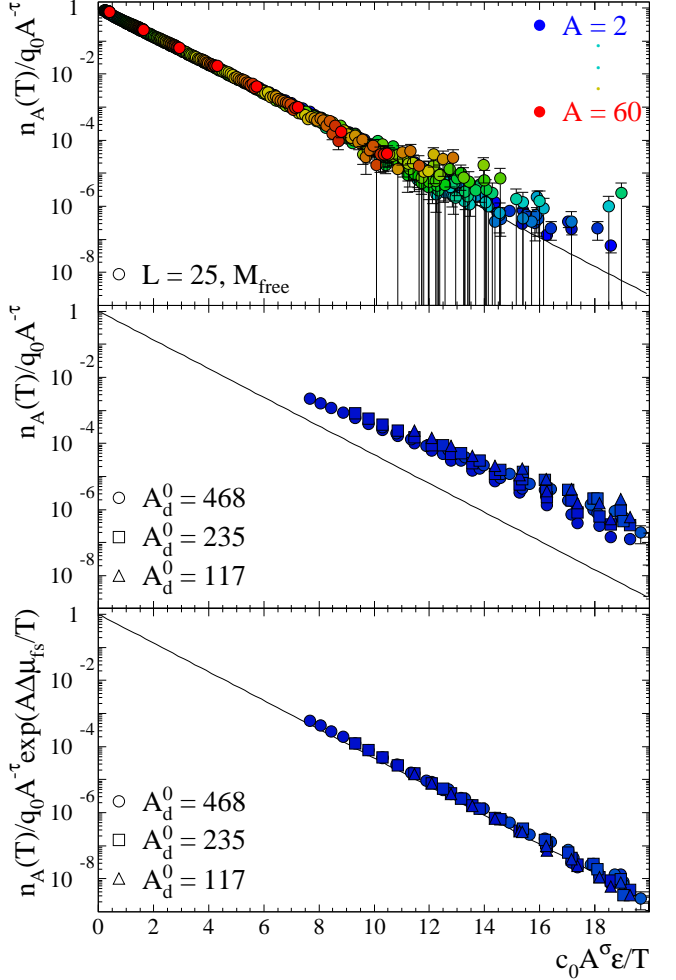


FIG. 3: [Color online] Same as Fig. 2 but for the  $d = 3$ ,  $L = 25$  periodic boundary condition simple cubic lattice.

TABLE II:  $\chi^2_\nu$  results for  $M_{\text{fixed}}$  calculations

$A_d^0 (d = 2)$	640	320	160
$\chi^2_\nu$ w/o complement	10.3	10.6	18.2
$\chi^2_\nu$ w complement	1.7	1.9	4.8
$A_d^0 (d = 3)$	468	234	117
$\chi^2_\nu$ w/o complement	14.8	25.9	7.9
$\chi^2_\nu$ w complement	1.5	5.4	838.6
	516.0	258.1	

468, 234 and 117, respectively.

To make a comparison between the scaling achieved the  $M_{\text{free}}$  clusters and the  $M_{\text{fixed}}$  clusters, we fit the  $M_{\text{free}}$  clusters with Eq. (1) with the free parameters  $T_c$ ,  $c_0$ ,  $\sigma$  and  $\tau$ ;  $q_0 = \zeta(\tau - 1)/2$ . Results are given in Table I and shown in top panels of figures 2 and 3. The values of the  $T_c$  and  $\tau$  returned by this procedure are within 1% of their established values. The value of  $c_0$  shows that all clusters are not perfect squares (cubes) in  $d = 2$  ( $3$ ) for

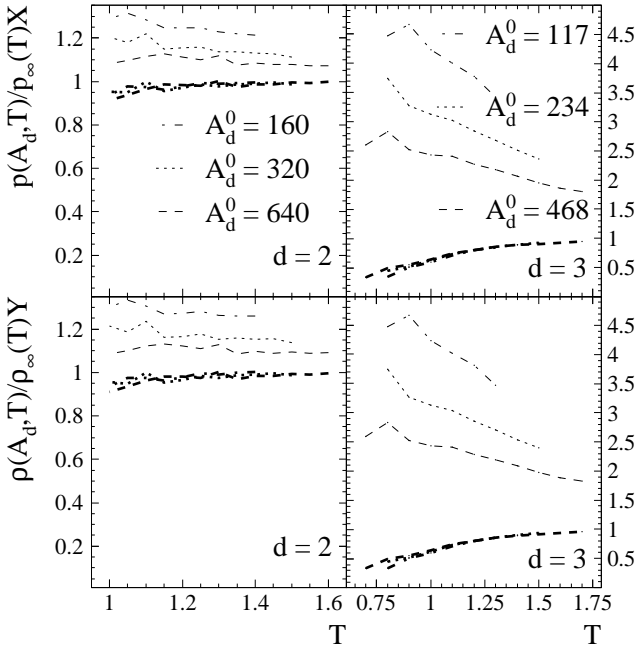


FIG. 4: Left (right) the normalized pressure and density of a vapor in coexistence with a drop  $A_d$  for  $d = 2$  (3). Thin [thick] lines show no complement results,  $X = Y = 1$  [complement results,  $X$  and  $Y$  from Eqs. (5) and (6)].

which  $c_0 = 8$  (12) [9, 20]. The value of  $\sigma$  are within 5% (15%) of their established values for  $d = 2$  (3). This level of inaccuracy arises from the geometrical shell effects [21].

Next we calculate  $\chi_\nu^2$  for the  $M_{\text{fixed}}$  clusters using Eq. (1) and Eq. (2) with parameters fixed to the Table I values. This procedure frees us as much as possible from the drawbacks of Fisher's model so we can concentrate on the effect of the complement. Results are given in Table II and shown in the middle panels (without complement: concentrations scaled as  $n_A(T)/q_0 A^{-\tau}$ ) and the bottom panels (with complement: concentrations scaled as  $n_A(T)/q_0 A^{-\tau} \exp[A\Delta\mu_{\text{fs}}/T]$ ) of figures 2 and 3. The  $M_{\text{fixed}}$   $\chi_\nu^2$  values for the calculation with the complement are an order of magnitude smaller than the results without the complement and the data collapse is better.

The middle and bottom panels of figures 2 and 3 show the major point of this paper: generalizing Fisher's model with the complement accounts for the finiteness of the liquid. The middle panels of figures 2 and 3 show that the  $M_{\text{fixed}}$  calculations do not scale as their  $M_{\text{free}}$  counterparts. The bottom panels of figures 2 and 3 show that when the complement effect is taken into account, the  $M_{\text{fixed}}$  calculations scale as their  $M_{\text{free}}$  counterparts.

We now confront the integrated quantities pressure  $p(A_d, T) = T \sum_A n_A(T)$  and density  $\rho(A_d, T) = \sum_A n_A(T)A$ . For  $A_d \gg A$  expanding  $\Delta\mu_{\text{fs}}$  gives

$$\Delta\mu_{\text{fs}} = 1 + A \left( \frac{\tau}{A_d} + \frac{\sigma c_0 \varepsilon}{T A_d^{1-\sigma}} \right) + \dots \quad (4)$$

This leads to

$$\begin{aligned} p(A_d, T) &\approx p_\infty(T) \exp \left[ \left( \frac{\tau}{A_d} + \frac{\sigma c_0 \varepsilon}{T A_d^{1-\sigma}} \right) \frac{\sum_A n_A^\infty(T) A}{\sum_A n_A^\infty(T)} \right] \\ &= p_\infty(T) X \end{aligned} \quad (5)$$

and

$$\begin{aligned} \rho(A_d, T) &\approx \rho_\infty(T) \exp \left[ \left( \frac{\tau}{A_d} + \frac{\sigma c_0 \varepsilon}{T A_d^{1-\sigma}} \right) \frac{\sum_A n_A^\infty(T) A^2}{\sum_A n_A^\infty(T) A} \right] \\ &= \rho_\infty(T) Y. \end{aligned} \quad (6)$$

For a vapor of monomers as  $A_d \gg \tau$  equations (5) and (6) yield the Gibbs-Thomson formulae [8].

Figure 4 shows the behavior of  $p(A_d, T)$  and  $\rho(A_d, T)$  for the  $M_{\text{fixed}}$  calculations compared to the bulk results. To free ourselves from finite lattice size effects  $p_\infty(T)$ ,  $\rho_\infty(T)$  and  $n_A^\infty(T)$  are determined from the  $M_{\text{free}}$  calculations. As expected  $p(A_d, T) > p_\infty(T)$  and  $\rho(A_d, T) > \rho_\infty(T)$  (thin lines in Fig. 4); i.e. the ratio in question is  $> 1$ . Accounting for the complement via equations (5) and (6) (using values in Table I) collapses results from all the calculations to a single line recovering the bulk behavior (thick lines in Fig. 4); i.e. the ratio in question is  $\sim 1$ . Deviations at low  $T$  are due to the increasing effects of monomers which have  $c_0 = 8$  (12) in  $d = 2$  (3).

A general approach in terms of the complement has been developed which allows one to account for finite liquid drop size effects and to extrapolate from finite to infinite systems. We have demonstrated the applicability of our method in the lattice gas model (Ising) calculations. This method can be immediately generalized to include other energy factors present in the nuclear case and can be used to infer the phase diagram of infinite symmetric nuclear matter from experimental nuclear data.

---

[1] M. Schmidt *et al.*, Phys. Rev. Lett. **86**, 1191 (2001).  
[2] M. D'Agostino *et al.*, Phys. Lett. B **473**, 219 (2000).  
[3] J. B. Elliott *et al.*, Phys. Rev. Lett. **88**, 042701 (2002).  
[4] L. Rayleigh, Philos. Mag. **34**, 94 (1917).  
[5] L. G. Moretto, *et al.*, Phys. Rev. C **66**, 041601(R) (2002).  
[6] M. E. Fisher, Rep. Prog. Phys. **30**, 615 (1969).  
[7] L. G. Moretto *et al.*, Phys. Rev. C **68**, 1602 (2003).  
[8] B. Krishnamachari *et al.*, Phys. Rev. B **54**, 8899 (1996).  
[9] C. M. Mader *et al.*, Phys. Rev. C **68**, 064601 (2003).  
[10] K. Binder *et al.*, Phys. Rev. B **9**, 2328 (1974).  
[11] A. E. Ferdinand *et al.*, Phys. Rev. **185**, 832 (1969).  
[12] D. P. Landau, Phys. Rev. B **13**, 2997 (1976).  
[13] D. P. Landau, Phys. Rev. B **14**, 255 (1976).  
[14] T. D. Lee and C. N. Yang, Phys. Rev. **87**, 404 (1952).  
[15] T. D. Lee and C. N. Yang, Phys. Rev. **87**, 410 (1952).  
[16] K. Binder, Z. Phys. B **43**, 119 (1981).  
[17] J. R. Heringa *et al.*, Phys. A **254**, 156 (1998).  
[18] J. B. Elliott *et al.*, nucl-th/0405042 (2004).  
[19] A. Coniglio and W. Klein, J. Phys. A **13**, 2775 (1980).  
[20] D. Stauffer, Int. J. Mod. Phys. C **10**, 809 (1999).  
[21] J. B. Elliott *et al.*, LBNL NSD Annual Report (2003).